



# Predicting the dominating factors during heat transfer in magnetocaloric composite wires

Maria Krautz<sup>a,\*</sup>, Lukas Beyer<sup>a</sup>, Alexander Funk<sup>a,b</sup>, Anja Waske<sup>a,b</sup>, Bruno Weise<sup>a</sup>, Jens Freudenberger<sup>a,c</sup>, Tino Gottschall<sup>d</sup>

<sup>a</sup> Institute for Complex Materials, Leibniz IFW Dresden, Helmholtzstr. 20, 01069 Dresden, Germany

<sup>b</sup> Bundesanstalt für Materialforschung und -prüfung (BAM), Berlin, Germany

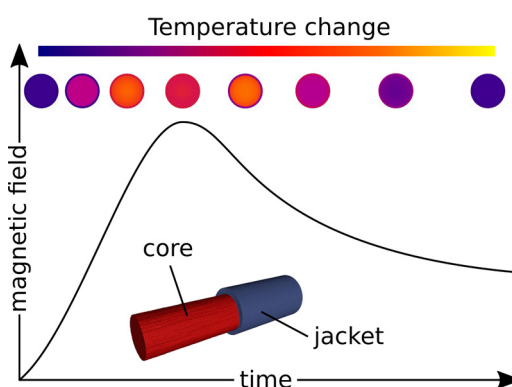
<sup>c</sup> Institute of Materials Science, Technische Universität Bergakademie Freiberg, Gustav-Zeuner-Str. 5, 09599 Freiberg, Germany

<sup>d</sup> Dresden High Magnetic Field Laboratory (HLD-EMFL), Helmholtz-Zentrum Dresden-Rossendorf, Dresden, Germany

## HIGHLIGHTS

- simultaneous monitoring of magnetic-field induced temperature change of magnetocaloric core and surrounding steel jacket
- 75% of the intrinsic  $\Delta T_{ad}$  in  $\text{La}(\text{Fe},\text{Co},\text{Si})_{13}$  can be used directly as  $\Delta T_{eff}$  at the jacket for field-frequencies of  $<2\text{Hz}$
- inverse thermal hysteresis of the core temperature change observed for field frequencies  $>10\text{Hz}$
- numerical simulations provide guidelines for the best choice of material combination in magnetocaloric composite wires

## GRAPHICAL ABSTRACT



## ARTICLE INFO

### Article history:

Received 14 April 2020

Received in revised form 19 May 2020

Accepted 26 May 2020

Available online 30 May 2020

### Keywords:

Heat transfer

Numerical simulation

Pulsed magnetic field

Composite

## ABSTRACT

Magnetocaloric composite wires have been studied by pulsed-field measurements up to  $\mu_0\Delta H = 10\text{ T}$  with a typical rise time of 13 ms in order to evaluate the evolution of the adiabatic temperature change of the core,  $\Delta T_{ad}$ , and to determine the effective temperature change at the surrounding steel jacket,  $\Delta T_{eff}$ , during the field pulse. An inverse thermal hysteresis is observed for  $\Delta T_{ad}$  due to the delayed thermal transfer. By numerical simulations of application-relevant sinusoidal magnetic field profiles, it can be stated that for field-frequencies of up to two field cycles per second heat can be efficiently transferred from the core to the outside of the jacket. In addition, intense numerical simulations of the temperature change of the core and jacket were performed by varying different parameters, such as frequency, heat capacity, thermal conductivity and interface resistance in order to shed light on their impact on  $\Delta T_{eff}$  at the outside of the jacket in comparison to  $\Delta T_{ad}$  provided by the core.

© 2018 The Authors. Published by Elsevier Ltd. This is an open access article under the CC BY license (<http://creativecommons.org/licenses/by/4.0/>).

## 1. Introduction

The need to develop novel cooling technologies to conventional refrigeration and air-conditioning is urgent in view of the growing energy

demand of the refrigeration sector and its growing contribution to climate change [1]. This factor is taken into account for example by the revised European F-gas regulation (No 517/2014) aiming for the successive reduction of fluorinated greenhouse gases “by 80–95% below 1990 levels by 2050” [2].

Magnetic refrigeration is a solid state cooling technology based on the magnetocaloric effect exhibited near the magnetic phase transition

\* Corresponding author.

E-mail address: [m.krautz@ifw-dresden.de](mailto:m.krautz@ifw-dresden.de) (M. Krautz).

of a material. Despite a huge number of prototypes have been developed during the last years as proof-of-concept, commercialization of magnetic refrigeration is not fully accomplished. The road map of Gottschall et al. summarizes the required magnetocaloric material properties and the obstacles that need to be tackled by the construction of a magnetic refrigerator to enhance the market opportunities of magnetic cooling [3]. An essential aspect is the shaping of the magnetocaloric materials into suitable heat exchanger geometries. To optimally exploit the cooling potential of the magnetocaloric material, the design of the heat exchanger geometry needs to satisfy two diametric requirements: Coarse structures ensure a low pressure drop over the working length of the heat exchanger while a high surface-to-volume ratio provided by small, porous structures is required at the same time to ensure an effective heat exchange. Since the most promising material families considered for room-temperature application are intermetallic phases, such as the  $\text{La}(\text{Fe}, \text{Si})_{13}$ -based or  $(\text{Mn}, \text{Fe})_2(\text{P}, \text{Si})$ -based alloys [4], the choice of shaping technologies for the manufacturing of optimally designed heat exchangers are limited. Apart from the simple geometries, such as loose powder beds and plane plates, more advanced shapes have been produced by extrusion [5], additive manufacturing [6] or tape casting [7,8]. These methods allow a high design flexibility, however, the required post-heat treatment leads to a severe reduction of mechanical integrity and in consequence cyclability. Several metal-bonded composites with different low-melting elements or alloys have been produced by hot-pressing, recently [9–13]. However, no filigrane structures were realized in these publications. In [14], composite wires with a magnetocaloric (active)  $\text{La}(\text{Fe}, \text{Co}, \text{Si})_{13}$ -core clad by a non-magnetocaloric (passive) austenitic steel jacket were produced by applying the powder-in-tube (PIT) process. This process was applied for the first time on a magnetocaloric material. Wires can serve as versatile building units for a variety of arrangements, such as parallel bundles, parallel and corrugated pin rows, or meshes, to make heat exchanger structures that comply the above mentioned trade-off between pressure loss and heat transfer. Moreover, the austenitic steel jacket prevents the magnetocaloric material to disintegrate during magnetic cycling and its corrosion is inhibited. Despite the unpromising mechanical properties of the magnetocaloric material, the composite wires were swaged down from 6 mm to 1 mm with a resulting steel jacket width of <0.1 mm. The resulting fraction of the core material in the composite wires is as large as 58 vol% which is close to the value of recently produced composite plates [15–17]. The entropy change after mechanical deformation during the PIT process is restored to the value of the reference sample by a short-time heat treatment. However, it is not trivial to study the heat flows within and out of such a wire in the fast magnetic-field-sweep rates that are typically used for magnetic refrigeration. In this article, the thermal-transport properties of magnetocaloric  $\text{La}(\text{Fe}, \text{Co}, \text{Si})_{13}$ -based composite wires are investigated by means of direct measurements of the adiabatic temperature change induced by a magnetic-field pulse in the core and simultaneously recording the temperature change at the outer surface of the steel jacket.

The results of the present study are divided into three parts: First, the field-dependent evolution of the adiabatic temperature change in field pulses of up to 10 T in  $\approx 13$  ms of the magnetocaloric  $\text{La}(\text{Fe}, \text{Co}, \text{Si})_{13}$ -core is discussed and compared to the  $\Delta T_{\text{ad}}$ - and  $\Delta S_T$ -profiles derived from quasi-static measurements. The second part considers the steel jacket as non-magnetocaloric heat sink. For this, pulsed-field measurements of the composite wire are presented to determine the influence of the steel jacket on the effectively usable temperature change for heat exchange in the magnetocaloric regenerator. Numerical simulations of the temperature profile during the field pulse are utilized to explain the process of thermal conduction within the  $\text{La}(\text{Fe}, \text{Co}, \text{Si})_{13}$  composite wire. Based on this, the third part is devoted to the numerical simulations of the achievable effective temperature change  $\Delta T_{\text{eff}}$  under different operational conditions and for different material combinations in order to identify the dominant thermal properties influencing thermal conduction processes in the composites.

## 2. Experiments and methods

The samples were prepared as described in Ref. [14], in which the successful application of the Powder-in-Tube process for  $\text{La}(\text{Fe}, \text{Co}, \text{Si})_{13}$ -based alloys is shown. The magnetocaloric powder was clad in a seamless steel tube and successively swaged to a diameter of 1 mm with a wall thickness of about 100  $\mu\text{m}$ . For the measurements, samples with a length of 8 mm were used, i.e. a complete composite as well as a sole core with removed steel jacket that served as reference. For the sole core reference, the jacket of the composite was ground off. The progress was monitored by X-ray computed tomography to ensure that no surrounding steel was left.

The adiabatic temperature change and the thermal behavior between core and jacket were investigated using a pulsed-field magnet. This measurement technique is based on the principle that a short, very strong current pulse generates a high magnetic field to which the sample is exposed [18]. The temperature change was measured by fine twisted type T thermocouples consisting of copper and constantan wires with a diameter of 25  $\mu\text{m}$  [19,20]. These thermocouples were attached to the samples as well as to the back of the sample holder at the reference point for temperature monitoring. The core sample that should be used as comparison to the wire was cut in half, the thermocouple was attached with silver-based epoxy and the two parts were glued together in order to achieve the largest possible contact area between the thermocouple and the sample surface.

The composite wire sample needed to be equipped with two thermocouples. Also the wire sample was halved and glued together with one thermocouple attached by silver-based epoxy in the center of the core, the second one was mounted on the outside of the jacket. The positioning of the thermocouples was verified by X-ray computed tomography. The resulting images can be found in the Supplementary information (Fig. S1). 2D images of the contact area of the inner and outer thermocouples are shown and the difference between them in terms of positioning at the magnetocaloric core and at the non-magnetic jacket is presented. Both samples were aligned with their longest axis along the field in order to minimize demagnetization effects. In order to control the temperature of the sample assembly, the holder was surrounded by a heater and its temperature was determined by a calibrated Pt100 resistance. After sample preparation and installation of the heater, the entire assembly was inserted into the measuring system and a high vacuum ( $p = 5 \times 10^{-5}$  mbar) was applied. Magnetic-field pulses were emitted for 2, 5 and 10 T in  $\approx 13$  ms. For each sample, six temperatures were measured around the magnetic transition temperature of the  $\text{La}(\text{Fe}, \text{Co}, \text{Si})_{13}$ -core in a range between 300...325 K. For each field and temperature step, two pulses - one in positive and one in negative field direction - were applied in order to average any interfering signal.

The specific heat in magnetic fields of 0, 2, 5 and 9 T was measured using a Physical Property Measurement System (PPMS) from Quantum Design. The calorimeter employs the relaxation method to derive the heat capacity [21]. From this data, the adiabatic temperature change  $\Delta T_{\text{ad}}$  and the isothermal entropy change  $\Delta S_T$  as a function of the initial temperature and the magnetic field were obtained by 3D interpolation (cf. Fig. S2). The smoothed surfaces resulting from this are illustrated in Fig. S2. The simulation of the magnetocaloric effect and thermal transport were performed using Comsol Multiphysics. Therefore, a 1D rotational symmetric model of the composite with similar dimensions was created. The local magnetocaloric effect  $dT = dT(r, T(r), H)$  was estimated for each magnetic-field increment based on the heat capacity results (see Supplementary information section IVB). For the  $\text{La}(\text{Fe}, \text{Co}, \text{Si})_{13}$  core, the density  $\rho = 7.4 \text{ g cm}^{-3}$  and thermal conductivity  $\lambda = 7.2 \text{ W m}^{-1} \text{ K}^{-1}$  were used [3] for the numerical simulations. The steel jacket was described with the parameters  $c_p = 510 \text{ J kg}^{-1} \text{ K}^{-1}$ ,  $\lambda = 40 \text{ W m}^{-1} \text{ K}^{-1}$ , and  $\rho = 7.75 \text{ g cm}^{-3}$ . Time-dependent simulations of the heat transfer have been done for the sole  $\text{La}(\text{Fe}, \text{Co}, \text{Si})_{13}$  core

and for the composite wire using different magnetic field profiles and material properties.

### 3. Results and discussion

#### 3.1. Magnetocaloric characterization of the $\text{La}(\text{Fe,Co,Si})_{13}$ -core in pulsed and static field

In Fig. 1, the typical progression of the sample temperature  $T_i$  upon a magnetic pulse is shown for the separated  $\text{La}(\text{Fe,Co,Si})_{13}$ -core material. The magnetocaloric effect occurs upon increasing magnetic field and the material heats up. The hysteresis occurring for pulses  $\mu_0 H > 2$  T can be understood by including the time profile of each field pulse (right in Fig. 1 and more detailed in Fig. S4). The field rate,  $\mu_0 dH/dt$ , during magnetization increases from 0.14 T/ms to 0.38 T/ms to 0.78 T/ms for 2, 5 and 10 T-field pulse, respectively. The increase of the hysteresis for high-field pulses, indicates a limited thermal exchange between the core and the thermocouple, whereas the coupling for the low-field pulse of 2 T is sufficient. On the contrary, during demagnetization, the rate of decay  $-\mu_0 dH/dt$  is exponential for each pulse and much slower than the magnetization rate, i. e. the cooling curve for the 2, 5 and 10 T pulse follow the same line. A detailed discussion on the pulsed-field rates can be found in [22].

The temperature-dependent adiabatic temperature change was derived from magnetic-field pulses at different  $T_i$  around the transition temperature of the core, as shown in Fig. 2. Additionally,  $\Delta T_{ad}$  calculated from heat capacity measurements is shown for comparison. Although these measurements are performed in static magnetic fields, the values of both methods correspond well indicating that the maximum  $\Delta T_{ad}$  in pulsed field is not affected by the thermal inertia of the core material. For the discussion of the influence of the surrounding steel on the effective adiabatic temperature change,  $\Delta T_{eff}$ , the full magnetocaloric characterization of the core material is essential. Based on the heat capacity measurements, the  $\Delta T_{ad}$ - and  $\Delta S_T$  profile of the  $\text{La}(\text{Fe,Co,Si})_{13}$ -core was simulated (Fig. S2). As can be seen in Fig. 2, the projection of the temperature-dependent  $\Delta T_{ad}$  for constant magnetic field in the simulation agrees well with the values calculated from the heat capacity measurements. This verifies the validity of the finite element model used for the numerical simulation.

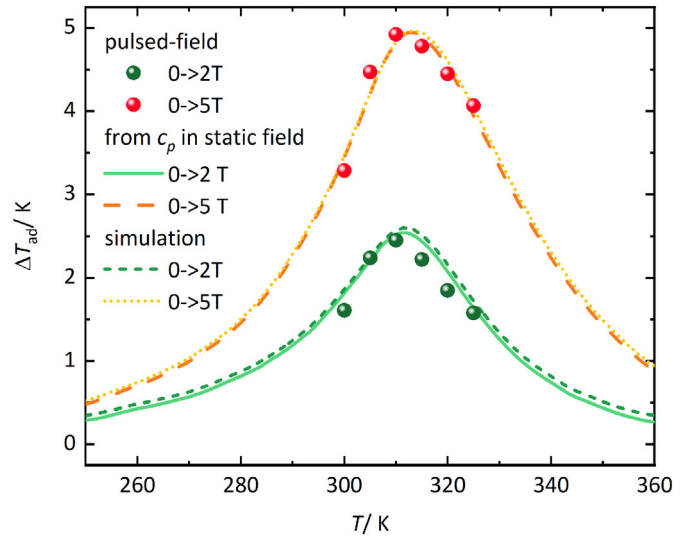


Fig. 2. Comparison of the adiabatic temperature change  $\Delta T_{ad}$  of the separated  $\text{La}(\text{Fe,Co,Si})_{13}$ -core determined indirectly by heat capacity measurements in static fields and directly from pulsed field measurements. The simulated  $\Delta T_{ad}$  at  $\mu_0 \Delta H = 2$  and 5 T is shown by the dashed and dotted curves, respectively.

#### 3.2. Temperature of the core and of the jacket in the PIT wire in pulsed magnetic fields

Considering the field-induced temperature change of the core, adiabatic conditions are no longer valid due to the thermal exchange between core and jacket. Hence,  $\Delta T$  rather than  $\Delta T_{ad}$  will be used during the following discussion.

In Fig. 3a, the time-profile of the temperature change induced by the magnetic-field pulse for the core and surrounding jacket is shown. As the magnetic field increases, the core exhibits the magnetocaloric effect and temperature increases by  $\Delta T$  (core). During this magnetization, the surrounding steel jacket is heated by the core, i. e. its temperature is increased by  $\Delta T_{eff}$  (jacket). However, the maxima of  $\Delta T$  and  $\Delta T_{eff}$  are shifted in time, indicating that a full heat transfer from core to jacket is not completed until the peak field is reached. This can be also concluded from Fig. 3b depicting the sample temperature change as a

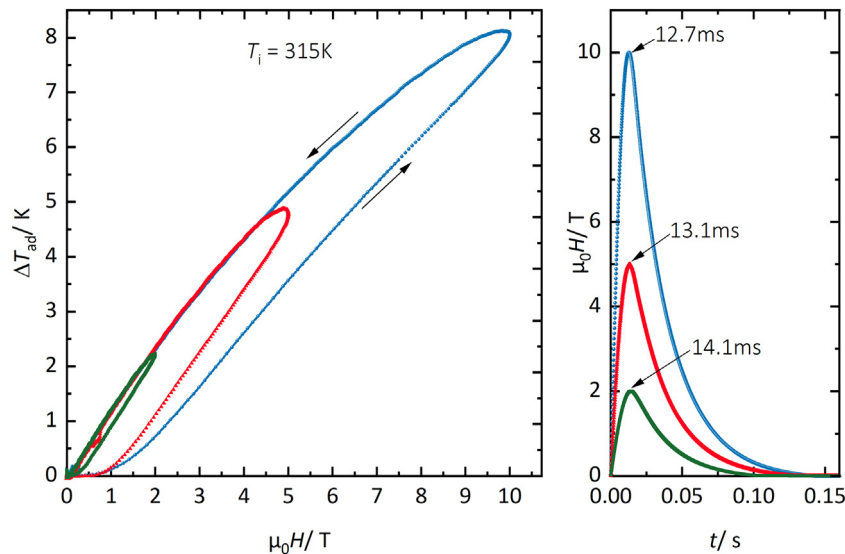
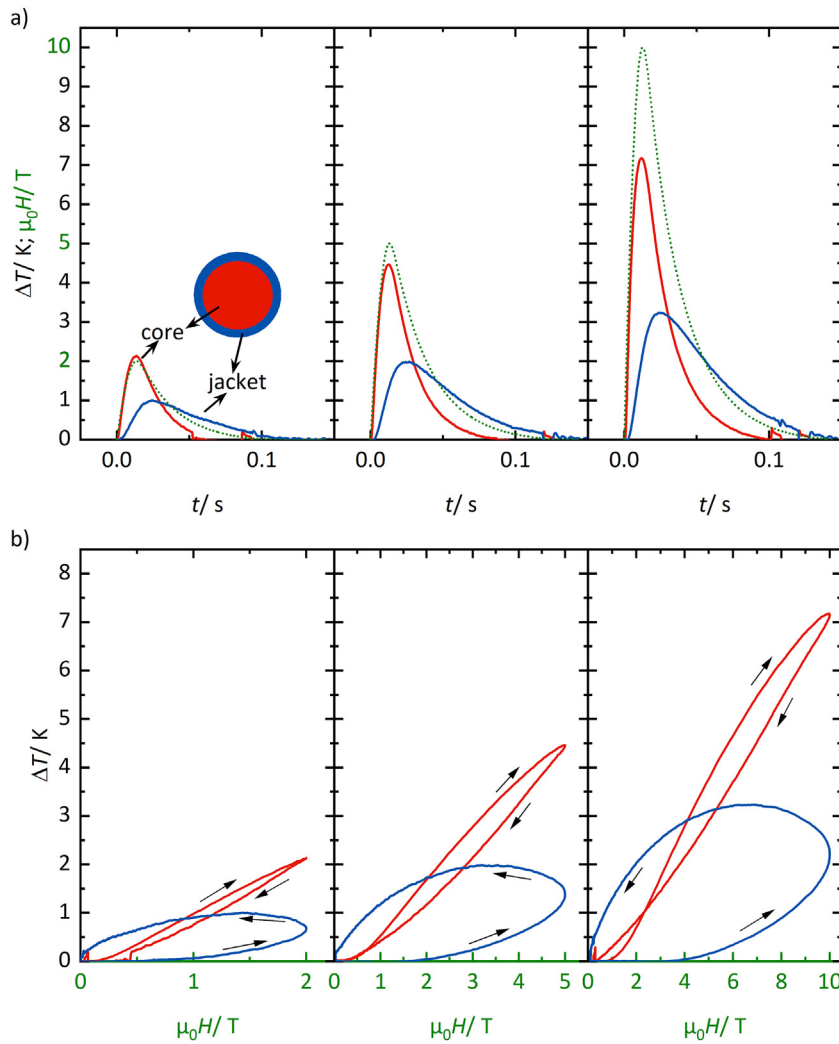


Fig. 1. Field-dependence of sample temperature change of the separated magnetocaloric core near the transition temperature as a result of  $\mu_0 \Delta H = 2, 5, 10$  T-field pulse (left). Time-profile of the magnetic-field pulses, labels indicate the rise time of the pulse (right).



**Fig. 3.** a) Evolution of the temperature change  $\Delta T$  of the magnetocaloric core and steel jacket during the magnetic-field pulse (illustrated by the green dotted line), b)  $\Delta T$  plotted as a function of magnetic field. The red and blue curves correspond to the core and jacket material, respectively. Shown data applies to  $T_i = 312$  K.

function of magnetic field instead, shown for better tangibility. The thermal coupling between the core and jacket results in a “reversed” hysteresis of the core.

In order to understand the behavior of the temperature change in the composite wires, numerical simulations were performed by including the thermal properties of the core and steel. From [23] it is known, that the thermal resistance,  $R_i$ , between the components plays a crucial role for their heat exchange. Therefore, thermal resistance was varied between  $R_i = 10^{-5} \dots 10^{-2} \text{ K m}^2 \text{ W}^{-1}$ . The best fit for the experimental data is obtained for the value of  $R_i = 10^{-4} \text{ K m}^2 \text{ W}^{-1}$ , which is three orders of magnitude smaller than the  $R_i$  in the polymer-bonded composites reported in [23]. In Fig. 4, the obtained simulated temperature change in pulsed fields is shown, in comparison to the measured data. Additionally to the core and jacket temperature evolution, the temperature at the interface can be drawn from the simulation (grey in Fig. 4). The largest difference between measurement and simulation is observed for the core material. This can be explained by the positioning of the thermocouple monitoring the core temperature change. As can be seen in S1, this thermocouple is located between two pieces of the PIT-wire which are not perfectly concentrically aligned to each other: On one side the thermocouple touches not only the wire core, but also the steel jacket, whereas the other side fully touches the magnetocaloric core. The signal from this thermocouple, therefore, is slightly influenced by the steel jacket. However, the full characteristics

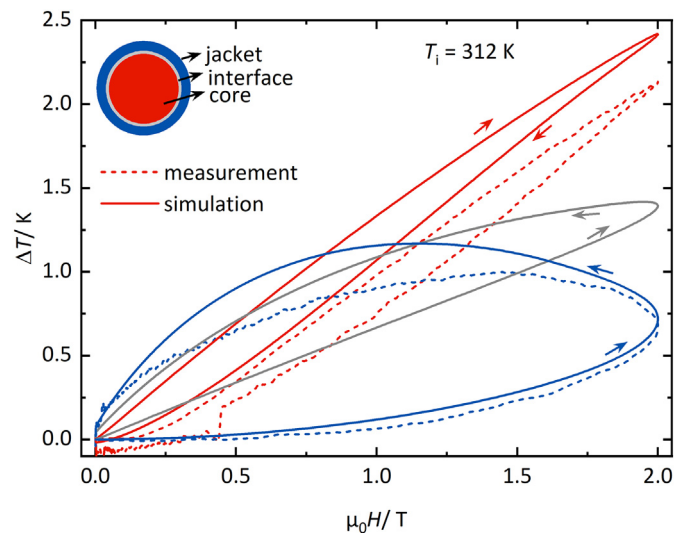


**Fig. 4.** Experiment and numerical simulation of the temperature change in the composite wire upon a magnetic-field pulse up to 2 T.

of the field hysteresis of both, the jacket and the core, are fully reproduced by the numerical simulations.

From these findings, it can be concluded that the understanding of the heat transfer mechanism between core and jacket is crucial to understand the remaining effective temperature change in the jacket. This would be the figure of merit to rate the performance of the powder-in-tube composite wires. In the following section, numerical simulations to determine the dominant parameters (material combination and frequency) on  $\Delta T_{\text{eff}}$  are shown for application relevant sinusoidal field changes.

### 3.3. Influence of thermal properties on $\Delta T$ in sinusoidal field

The results of the finite element analysis perfectly describe the observations of the experiments despite the short duration of the magnetic pulse of only a few milliseconds. For this reason, it is appropriate to adapt our model to other magnetic-field profiles, at least for timescales in the order or lower than the pulsed-field experiment. For the sake of simplicity, a sinusoidal field profile was chosen as it is created by the opposing rotation of two nested Halbach magnets [22]. In Fig. 5a, the simulated temperature change of the core (solid lines) and jacket (dashed lines) for a 2 T pulse and sinusoidal field profiles with various frequencies are illustrated. As discussed above, the temperature change of the jacket is lagging behind the core in the pulsed field experiments because only a limited amount of heat can be transferred to the outside of the composite. However, this allows the core to achieve a larger temperature change. If the magnetic field is applied slower, the jacket can follow faster, which reduces the maximum  $\Delta T$  of the core. This effect becomes apparent when comparing the temperature dependencies for field frequencies of  $f = 2.5, 1$  and  $0.5$  Hz in Fig. 5a. It can be seen that the respective curves for core and jacket are getting closer the more time is available for the heat exchange. It should be noted that the magnetic field is acting with  $B(t) = B_0|\sin(2\pi ft)|$  on the sample meaning that for a  $f = 2.5$  Hz the composite is magnetized and demagnetized 5 times each second.

If the temperature change in the respective maximum field is considered, the following frequency dependence as shown in Fig. 5b is obtained. For low frequencies, the temperature change of the core and jacket can be considered to be equal. However, it can be seen that splitting occurs at frequencies above 1 Hz. This indicates that the sample can complete two field cycles per second. In Fig. 5b, also the temperature change at the interface is plotted. This shows that a significant temperature gradient builds up at larger frequencies. Videos of the time-

dependent simulation results can be found in the Online supplementary material.

In the following, the influence of the jacket material on the composite performance is discussed. This is summarized in Fig. 6. The temperature change of the core, the jacket, and the interface depending on the volumetric heat capacity of the jacket for a sinusoidal magnetic field profile with a maximum field of 2 T and a frequency of 2.5 Hz is plotted in Fig. 6a. The thermal conductivity and the contact resistance remain unchanged. For the limit case of a negligible heat capacity of the jacket, the temperature change approaches the maximum possible  $\Delta T$  of about 2.42 K. However, if an ever increasing heat capacity is assumed, the temperature change on the outside and also of the core material is reduced, since the jacket acts as a heat load. Several materials are given with their volumetric heat capacity in Fig. 6a for comparison. It is found that steel is not the best choice as a jacket material in terms of performance, e.g. copper and aluminium only lead to little enhanced thermal coupling of the composite. However, the manufacturability using the powder-in-tube process must be taken into account, which is why material properties such as strength, ductility and temperature stability must be suitable as well. Steel is ideally suited in this context. However, the performance can be further improved by reducing the thermal load while further reducing the thickness of the jacket.

Despite this, the influence of thermal conductivity is investigated (Fig. 6b). For this, the heat capacity of steel is utilized and the interface resistance is  $R_i = 10^{-4} \text{ K m}^2 \text{ W}^{-1}$  as before. It can be seen that the temperature changes are unaffected by a change of the high thermal conductivity of the jacket being typical for metals. Instead, only below  $\lambda = 1 \text{ W m}^{-1} \text{ K}^{-1}$  as for polymer materials such as PTFE, a decisive reduction of the usable temperature change on the outside of the tube is observed. This shows, however, that at least for metallic jacket materials, the thermal conduction is not the limiting factor that determines the performance of the composite.

Finally, the role of the thermal contact resistance of the interface between the active  $\text{La}(\text{Fe},\text{Co},\text{Si})_{13}$  core and the passive steel jacket is discussed. This is illustrated in Fig. 6c. For small resistances of  $R_i < 10^{-4} \text{ K m}^2 \text{ W}^{-1}$ , heat can penetrate to the outside almost without hindrance. A temperature gradient can therefore not build up at all. However, if the thermal resistance at the contact surface increases, e.g. by gaps and pores, the temperature change of the jacket is significantly reduced. That can even go to the point that for values of  $R_i = 10^{-2} \text{ K m}^2 \text{ W}^{-1}$  and higher, as described for epoxy-bonded composites [23], the core is virtually isolated from the outside by the polymer. This shows that the nature of the interface and its permeability for heat is the decisive factor for heat conduction. To summarize, it can be concluded, that the presented composite wires are suitable for typical

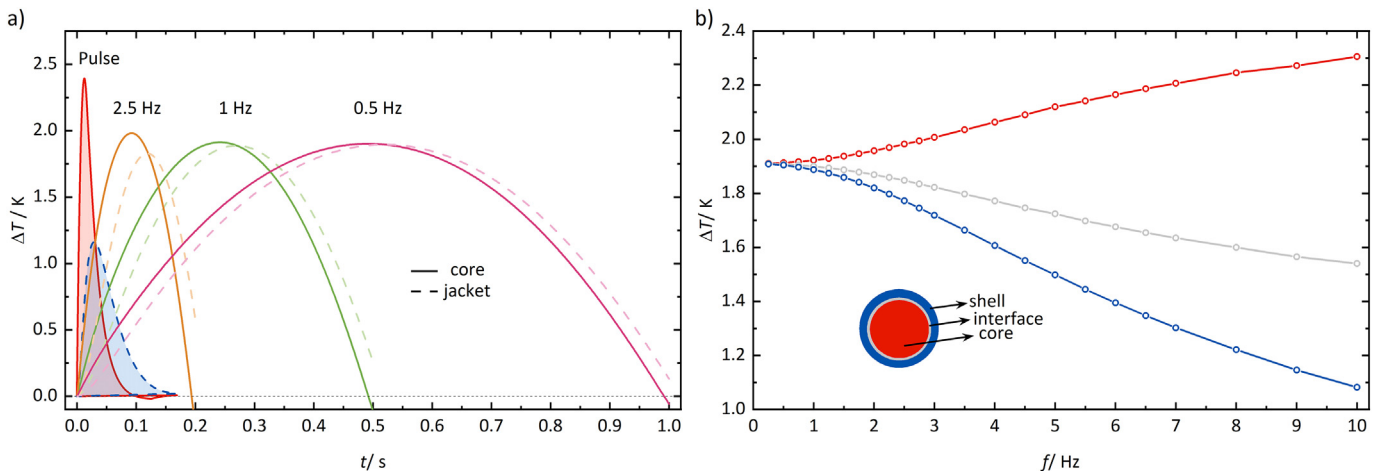
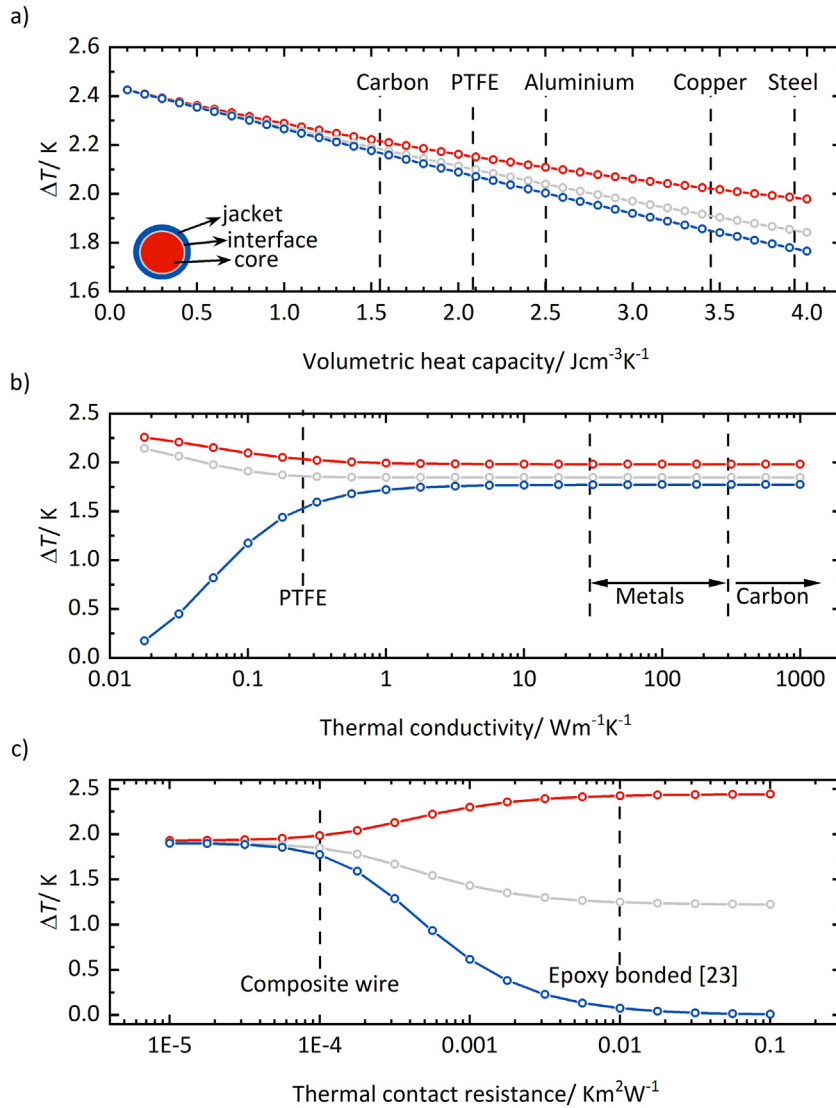


Fig. 5. a) Resulting temperature change in the core ( $\Delta T$ ) and steel jacket ( $\Delta T_{\text{eff}}$ ) when the magnetic field is applied with different time scales, b) summary of resulting  $\Delta T$  and  $\Delta T_{\text{eff}}$  for different operation frequencies. The field change corresponds to 2 T at a starting temperature of  $T_i = 312$  K.



**Fig. 6.** Resulting  $\Delta T$  and  $\Delta T_{eff}$  when different jacket materials are combined with  $La(Fe,Co,Si)_{13}$  as core: a) Influence of volumetric heat capacity, b) thermal conductivity and c) interface thermal resistance.

operation conditions of up to five field cycles, since the effectively usable temperature change,  $\Delta T_{eff}$ , at the jacket in  $f = 2.5$  Hz is 75% of the temperature change that occurs intrinsically in  $La(Fe,Co,Si)_{13}$  under adiabatic conditions (cf. Figs. 2 and 5a).

#### 4. Summary and conclusions for the design of magnetocaloric composites

The findings of the presented study are two-fold: First, the performance of a particular material combination is evaluated by pulsed-field measurements and combined numerical simulations on  $La(Fe,Co,Si)_{13}$ /steel wires prepared by the PIT-process. The second aspect comprises an extended view on alternative jacket materials to replace the austenitic steel. Results of numerical simulations of  $\Delta T$  and  $\Delta T_{eff}$  are gained from the variation of different material parameters, spanning several orders of magnitude in order to comprise all material classes in debate as potential jacket materials.

Conclusions for  $La(Fe,Co,Si)_{13}$ /steel wires as presented in [14]:

- $\Delta T_{eff}$  at the outside of the wires and  $\Delta T$  of the core are equal up to two field cycles per second

- above two field cycles, the maximum  $\Delta T_{eff}$  is delayed and hence reduced in comparison to  $\Delta T$  of the core
- $\Delta T_{eff}$  is governed by the heat capacity of the steel jacket, but not by the thermal conductivity due to the thickness of the jacket of only  $\approx 0.1$  mm
- in pulsed field (at operation frequencies  $> 10$  Hz) an inverted hysteresis of  $\Delta T$  of the core is observed due to the delayed heat exchange between core and jacket.

With respect to alternative jacket materials the following conclusions can be drawn:

- considering volumetric heat capacity instead of mass-related heat capacity is recommended to discuss the effectiveness of the passive matrix material
- as the thickness of the jacket is small ( $\approx 0.1$  mm), the effective adiabatic temperature change,  $\Delta T_{eff}$ , is almost independent of the heat conductivity of a given metal, e.g. Cu only lead to 5% enhancement of  $\Delta T_{eff}$  due to slightly reduced volumetric heat capacity compared to steel

- bonding between passive and active material is crucial for heat exchange and resulting  $\Delta T_{\text{eff}}$  (low thermal interface resistance).

These findings affect the materials choice and can be generalized to all magnetocaloric composites so far: Instead of varying the matrix material, e.g. by using metal-loaded polymer in plates or copper as jacket material for wires, the focus should lie on the reduction of the volumetric amount of the passive matrix material. The following directives help to prioritize the optimization factors for future composites:

1. Reduction of the volume fraction of passive matrix material
2. Deployment of magnetocaloric material with large  $\Delta T_{\text{ad}}$  to compensate losses due to the passive matrix
3. Avoid gaps at the interface between matrix and magnetocaloric material, ideal would be a chemical bonding.

It is to note, that such a generalizing study can also help to find promising material combinations for other applications of magnetocaloric materials, such as for field switches in thermomagnetic generator devices, although specific target figures might be opposite.

Supplementary data to this article can be found online at <https://doi.org/10.1016/j.matdes.2020.108832>.

### CRedit authorship contribution statement

**Maria Krautz:** Conceptualization, Methodology, Resources, Supervision, Writing - original draft, Writing - review & editing. **Lukas Beyer:** Methodology, Writing - original draft, Writing - review & editing. **Alexander Funk:** Methodology, Writing - review & editing. **Anja Waske:** Methodology, Writing - review & editing. **Bruno Weise:** Methodology, Writing - original draft, Writing - review & editing. **Jens Freudenberger:** Methodology, Writing - review & editing. **Tino Gottschall:** Conceptualization, Methodology, Resources, Supervision, Writing - original draft, Writing - review & editing.

### Declaration of competing interest

The authors declare that they have no known competing financial interests or personal relationships that could have appeared to influence the work reported in this paper.

### Acknowledgments

The authors gratefully acknowledge experimental support of Dirk Seifert from Institute for Complex Materials, IFW Dresden. This work has been financially supported by the German Research Foundation in the framework of SPP1599 "Ferroic Cooling" under grant WA3294/3-2

(A.W.), by the Germany Federal Ministry for Economic Affairs and Energy under the project number 03ET1374B (M.K., L.B.), the Helmholtz Association via the Helmholtz-RSF Joint Research Group with the Project No. HRSF-0045 (T.G.), and the HLD at HZDR, a member of the European Magnetic Field Laboratory (EMFL).

### Data availability statement

The raw and processed data required to reproduce these findings will be made available upon request.

### References

- [1] D. Coulomb, J.-L. Dupont, The Impact of the Refrigeration Sector on Climate Change, 11.2017.
- [2] Regulation (EU) No 517/2014 of the European Parliament and of the Council 20.5.2014.
- [3] T. Gottschall, K.P. Skokov, M. Fries, A. Taubel, I. Radulov, F. Scheibel, D. Benke, S. Riegg, O. Gutfleisch, Adv. Energy Mater. 9 (2019) 1901322.
- [4] V. Franco, J. Blázquez, J. Ipus, J.Y. Law, A. Conde, Prog. Mater. Sci. 93 (2018) 112.
- [5] S. Wieland, F. Petzoldt, J. Alloys Compd. 719 (2017) 182.
- [6] J.D. Moore, K. Morrison, K.G. Sandeman, M. Katter, L.F. Cohen, Appl. Phys. Lett. 95 (2009) 252504(3).
- [7] C.R.H. Bahl, D. Velázquez, K.K. Nielsen, K. Engelbrecht, K.B. Andersen, R. Bulatova, N. Pryds, Appl. Phys. Lett. 100 (2012), 121905.
- [8] M. Krautz, M. Beyer, C. Jäschke, L. Schinke, A. Waske, J. Seifert, Crystals 9 (2019) 76.
- [9] P. Wenkai, C. Yungui, T. Yongbai, Z. Lingtong, G. Huaqiang, Rare Metal Mater. Eng. 46 (2017) 2384.
- [10] X. Dong, X. Zhong, D. Peng, J. Huang, H. Zhang, D. Jiao, Z. Liu, R. Ramanujan, J. Alloys Compd. 737 (2018) 568.
- [11] D.R. Peng, X.C. Zhong, J.H. Huang, H. Zhang, Y.L. Huang, X.T. Dong, D.L. Jiao, Z.W. Liu, R.V. Ramanujan, MRS Commun. 8 (2018) 1216–1223.
- [12] Y. Ouyang, H. Zhang, M. Zhang, J. Liu, G. Yu, Z. Liu, J. Alloys Compd. 804 (2019) 49.
- [13] M. Zhang, Y. Ouyang, Y. Zhang, J. Liu, J. Alloys Compd. 823 (2020) 153846.
- [14] A. Funk, J. Freudenberger, A. Waske, M. Krautz, Mater. Today Energy 9 (2018) 223.
- [15] B. Pulko, J. Tušek, J.D. Moore, B. Weise, K.P. Skokov, O. Mityashkin, A. Kitanovski, C. Favero, P. Fajfar, O. Gutfleisch, A. Waske, A. Poredoš, J. Magn. Magn. Mater. 375 (2015) 65.
- [16] I. Radulov, D.Y. Karpenkov, K. Skokov, A.Y. Karpenkov, T. Braun, V. Brabänder, T. Gottschall, M. Pabst, B. Stoll, O. Gutfleisch, Acta Mater. 127 (2017) 389.
- [17] D. Goswami, K. Anand, P.P. Jana, S.K. Ghorai, S. Chattopadhyay, J. Das, Mater. Des. 187 (2020), 108399.
- [18] T. Herrmannsdörfer, H. Krug, F. Pobell, S. Zherlitsyn, H. Eschrig, J. Freudenberger, K.H. Müller, L. Schultz, J. Low Temp. Phys. 133 (2003) 41.
- [19] F. Scheibel, T. Gottschall, K. Skokov, O. Gutfleisch, M. Ghorbani-Zavareh, Y. Skourski, J. Wosnitza, Ö. Çakır, M. Farle, M. Acet, J. Appl. Phys. 117 (2015), 233902.
- [20] T. Gottschall, M.D. Kuz'min, K.P. Skokov, Y. Skourski, M. Fries, O. Gutfleisch, M.G. Zavareh, D.L. Schlagel, Y. Mudryk, V. Pecharsky, J. Wosnitza, Phys. Rev. B 99 (2019), 134429.
- [21] J.S. Hwang, K.J. Lin, C. Tien, Rev. Sci. Instrum. 68 (1997) 94.
- [22] T. Gottschall, K.P. Skokov, F. Scheibel, M. Acet, M.G. Zavareh, Y. Skourski, J. Wosnitza, M. Farle, O. Gutfleisch, Phys. Rev. Appl. 5 (2016), 024013.
- [23] K. Sellschopp, B. Weise, M. Krautz, F. Cugini, M. Solzi, L. Helmich, A. Hütten, A. Waske, Energy Technol. 6 (2018) 1448.